

# MULTI-FREQUENCY FEEDS FOR EARTH OBSERVATION APPLICATIONS

L. Costes<sup>1</sup>, JC. Orlhac<sup>1</sup>, JM. Goutoule<sup>1</sup>, JP. Adam<sup>2</sup>, Y. Beniguel<sup>2</sup>, A. Berthon<sup>2</sup>, M. van der Vorst<sup>3</sup>

<sup>1</sup>EADS Astrium, France, laurent.costes@astrium.eads.net

<sup>2</sup>IEEA, France, beniguel@ieea.fr

<sup>3</sup>ESA, The Netherlands, maarten.van.der.vorst@esa.int

**Keywords:** dual-frequency feed, FSS, waveguide diplexer, millimetre wave, corrugated horn.

## Abstract

In preparation of the EUMETSAT post-EPS user consultation process the European Space Agency has studied future operational meteorological microwave missions including the EGPM (European contribution to the Global Precipitation Measurement mission) type requirements at Pre-Phase A level. These requirements include a dual 54/119 GHz channel capability.

ASTRIUM has been selected by ESA to carry out the Multi-Frequency Feeds for Earth Observation Applications Study. The main objective of this activity is to design and test a defocused dual-frequency horn, operating at frequencies 54 and 119 GHz, to be combined with an offset reflector. To derive the required precipitation products from the measurements, both frequency bands (54 and 119 GHz) have to be optimised for a footprint overlap of at least 90% of the largest footprint and for high beam efficiency (> 95%).

The Dual-Frequency Feed (DFF) includes the dual-frequency horn and the diplexer for 54/119 GHz channels separation. ASTRIUM, as Study responsible, is in charge of the overall antenna engineering, including the reflector, the diplexer design and the DFF manufacturing and test. IEEA is responsible for the horn design. The horn shall exhibit high level performance in both 54 and 119 GHz frequency bands (VSWR, cross-polar, sidelobes) whilst the diplexer shall discriminate both channels with high level isolation (>40 dB) and with minimum insertion loss (<0.15 dB at 119 GHz).

## 1 Introduction

This document presents the design activities performed by IEEA on the dual-frequency horn and the “waveguide diplexer with integrated FSS (\*)”, an original diplexer design proposed and studied by ASTRIUM. The DFF principle is shown in Figure 1. For final performance assessment, the antenna radiation patterns at reflector level are also derived using the predicted DFF radiation patterns.

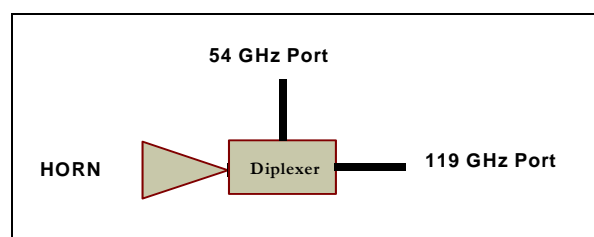
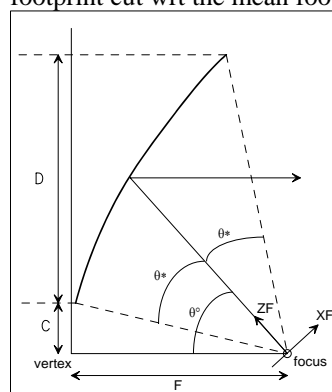


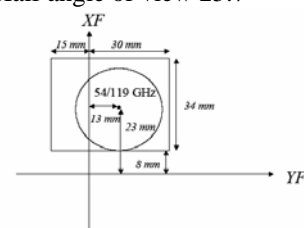
Figure 1: Dual-Frequency Feed (DFF) block diagram

## 2 Requirements

At antenna level, i.e. including reflector, the -3dB footprints shall be identical for both 54 and 119 GHz frequency bands. As there are several feeds to be accommodated within the instrument feed cluster, the DFF is not located at the reflector focus but shifted around 25 mm as shown in figure 2. This defocused feed location will produce some distortion on the antenna radiation pattern. As a consequence, the footprints will not be perfectly circular but will stay in the limit of 20% from a circular shape (ratio of maximum and minimum footprint cut wrt the mean footprint value).



Projected diameter 1200mm  
Focal length 1100mm  
Clearance 400mm  
Offset angle 46.3°  
Half angle of view 25.7°



Centre frequency	52.5 GHz	118.75 GHz
Bandwidth	± 2750 MHz	± 9000 MHz
Polarisation	Both H or both V	
Full Half Power Beamwidth (FHPBW)	< 0.58°	< 0.58°
FHPBW circular shape	< 20 %	< 20 %
Footprint overlap	> 90 %	
Beam efficiency	> 95 %	
Cross Polarisation	< -25 dB	

Figure 2: Antenna geometry & requirements

### 3 Horn design and performance

This section is dedicated to the design of the dual-frequency horn. A particular attention has been put on the footprint overlap at both operating frequencies which was found to be the most difficult requirement to meet.

Several horn concepts have been investigated:

- Smooth-walled horn
- Piecewise linear profile horn (kind of “Potter” horn)
- Corrugated horn, single and dual-depth
- Horn/lens combination

Smooth-walled and corrugated horns have been studied in more details as they showed the more promising performance. After general considerations on the design optimisation procedure, the best horn concept and performance is presented.

#### 3.1 Footprint overlap analysis

The aim of this part is the theoretical analysis of the footprint overlap in order to identify the constraints at horn level.

The effect of the feed radiation characteristics (amplitude and phase) on the beamwidth of the entire antenna has been studied. It was shown in [2] that the effect of the feed displacement may be complex and depends on its amplitude pattern.

In order to simplify the problem, the centre of the feed aperture is located at the focus point of the reflector. The feed is reduced to a source point located at the phase centre. The amplitude pattern is supposed identical in both principal planes. It is defined by  $\theta_{3dB}$ , one-half of the full half-power beamwidth. The amplitude pattern is then simplified as follows:

$$C(\theta) = \cos(\theta)^q \quad \text{with} \quad q = -0.15 / \log(\cos(\theta_{3dB})) \quad (1)$$

The Figure 3 presents the comparison between the real radiation patterns and this simplified formulation. The example shown is the corrugated horn design that leads to the best footprint overlap. This horn will be presented further in the document. The validity of the simplified formulation decreases with the amplitude level.

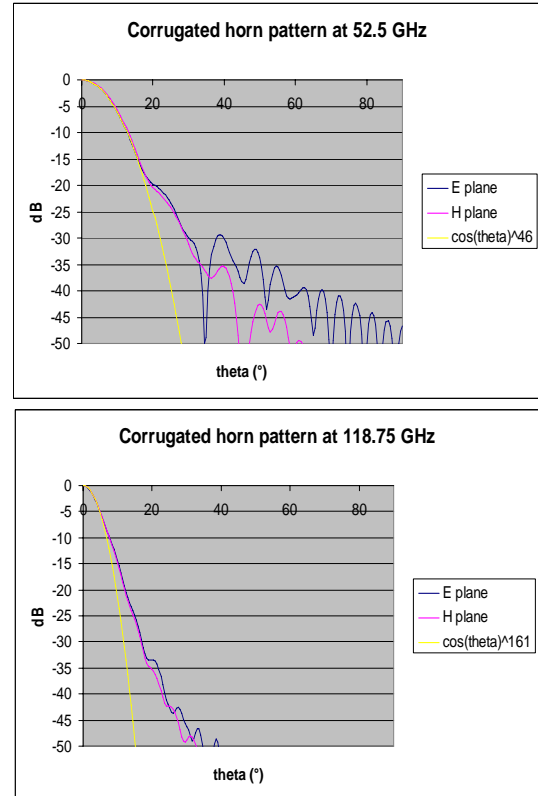


Figure 3: Radiation patterns of the corrugated horn and simplified  $\cos(\theta)^q$  pattern (yellow)

An interesting feature is shown in Figure 4: the position of the phase centre does not affect the beamwidth if it is close enough to the aperture plane (about  $<0.01$  m at 52.5 GHz and  $<0.02$  m at 118.75 GHz).

As a result, a design objective could be to reach a particular feed beamwidth (for example  $7^\circ$  at 52.5 GHz and  $3^\circ$  at 118.75 GHz) with only a maximum limit for the position of the phase centre. In other words, the constraints would be strong only on the amplitude pattern.

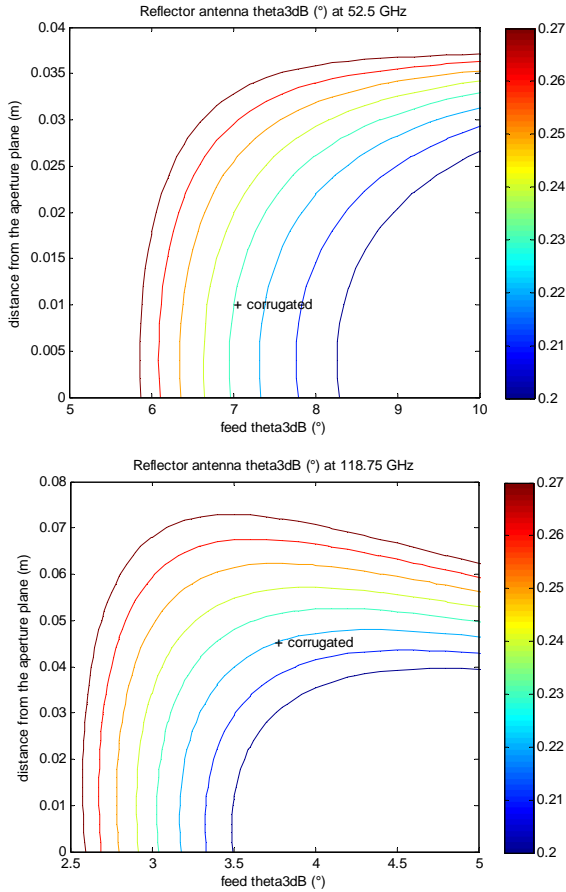


Figure 4: Isolevels of the reflector antenna half-power beamwidth at 52.5 GHz (top) and 118.75 GHz (bottom), as a function of the feed radiation characteristics. The position of the best feed design is also indicated

### 3.2 Horn design procedure

Once an initial dual frequency horn design is found, the design parameters are optimized to reach all requirements. Two existing optimizers were tested: a direct search complex algorithm and a quasi-Newton method with a finite-difference gradient. The obtained results and the number of design evaluations (including the finite-difference gradient) are equivalent.

For all the computed parameters  $Y$ , the cost function is defined as follows:

$$F = \sum_i \text{coeff}(i) * (Y_{\text{computed}}(i) / Y_{\text{objective}}(i) - 1)^2 \quad (2)$$

Since the parameters  $Y$  are normalized in this form, parameters of different physical nature can be used in the same cost function (VSWR, far field pattern, cross polarization, phase center location, footprint overlap...). The coefficients allow enhancing some parameters with respect to the others.

The feed is evaluated with the IEROS software (IEEA software) based on the Method of Moments (MoM) for rotationally symmetric structures [2]. For each iteration, the feed is evaluated at 52.5 GHz and 118.75 GHz.

The reflector can be included in the optimization process. However, the evaluation of the entire antenna needs more CPU time. In addition, bad convergence was observed if the reflector is taken into account. For this reason, this approach was used mainly if the initial design is not too far from the specifications. That was the case for the corrugated horn that has been designed.

### 3.3 Horn design analyses & selection

Two kinds of horns have been considered: smooth-walled and corrugated horn.

Because of the low cross-polarization required at feed level, less than -30 dB, an acceptable smooth-walled horn must be a multimode horn. One of the simplest multimode horns is the Potter horn. However, a Potter horn supports only a single narrow band [5] and therefore more complex multimode horns have to be considered. While the Potter horn is based on a radial step, there are other ways to generate higher modes, like for instance slope or curvature discontinuities. These designs are analysed in the following sections.

#### The spline profile

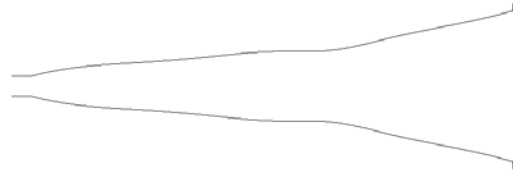


Figure 5: Spline profile horn

It was shown in [4] that a spline profiled horn may provide good radiation characteristics on a wide band. The design method described in [4] has been applied to design a dual-band spline profiled horn. Many different lengths of the launching sections, numbers of spline points and cost function coefficients were tested. The specified beam pattern envelopes were hardly reached.

#### The Piecewise linear profile

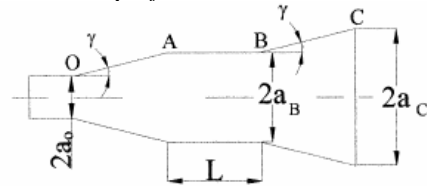


Figure 6: Piecewise linear profile horn

According to [3], a piecewise linear profile horn could have a dual band capability. The proposed horn designed in [3] works at 19 GHz and 29 GHz (these center frequencies are closer than in the present work). The design method in [5] needs an in-depth analysis of the higher modes generation process. In order to reduce the design time, a simpler approach was used. The starting design is a simple single band multimode horn deduced from [6]. This simple multimode horn is expected to have dual-band capability, like in [7]. Its geometrical parameters are then optimized for pattern shaping at both operating frequency.

### Dual-depth corrugated horn

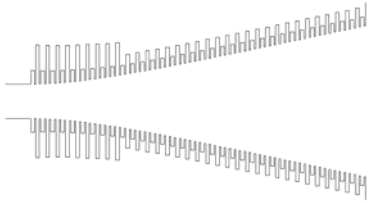


Figure 7: Dual-depth corrugated horn

Dual-depth corrugated horns should have the same low levels of cross polarization in two distinct frequency ranges. The HE<sub>11</sub> mode is the preferred mode of propagation. In order to avoid the EH modes, the ratio of the depths of the two slots is limited to a very defined ratio (EH is the second set of solutions to the boundary conditions, but can not achieve the smooth radial distribution desired for corrugated horns). A dual-depth corrugated feed horn can be used when the ratio of the centre frequencies of the operating bands is roughly between 1:1.3 and 1:2. According to [8], below this ratio single-depth will work, while above this ratio it is possible to use a single-depth corrugated horn with a slot working at two distinct frequencies. In our study, the center frequency ratio is 1:2.26, which should be unreachable for a dual-depth corrugated horn. However, some dual-depth corrugated horn designs were tested.

We started from a dual-depth corrugated horn directly deduced from [9], where the frequency ratio is 1:1.47, which is suited for the use of such a horn. This design was extended to a frequency ratio of 1:2.26. As expected, the cross polarization was too high for one of the operating frequencies (29.65 GHz). However, this test leads to an interesting feature: like in [9], the higher band slots operate at  $3\lambda/4$ . It appears that this value is close to  $\lambda/4$  in the lower band (all the slots have almost the same depth in the horn). This property has been used for the design of the single depth corrugated horn.

### Single-depth corrugated horn

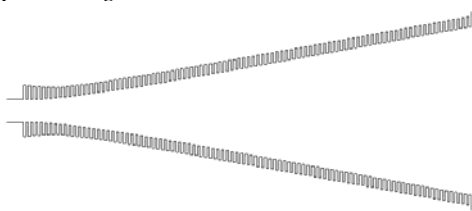


Figure 8: Single-depth corrugated horn

The single depth horn is based on the following idea: the slot depth is about  $3\lambda/4$  at 118.75 GHz and about  $\lambda/4$  at 52.5 GHz. The full offset reflector antenna is simulated at each iteration. However, to reduce the secondary radiation pattern computation time and to simplify the beamwidth computation, no defocusing was considered: the center of the horn aperture was located at the reflector focus. The degradation induced by the defocusing is small enough to justify this simplification.

Several profiles were considered: hyperbolic and Gaussian (formed with 2 hyperbolic profiles, or based on a sinusoid). The best overlap has been obtained with a hyperbolic profile.

Among all the investigated designs the single-depth corrugated horn has shown the best performance.

A smooth-walled horn generates and combines several modes. The generation and the propagation of each mode is frequency dependent: since the centre frequencies are very distinct, the multimode behaviour is probably different in the lower and in the higher band. In addition, the mode combination has to provide a low cross-polarization and a particular radiation pattern (for footprint overlap) at the same time.

On the contrary, there are fewer constraints on the corrugated horn, since the HE<sub>11</sub> mode provides naturally a low cross-polarization level. The corrugated horn provides quite easily a good footprint overlap and its size is shorter than the smooth-walled horns.

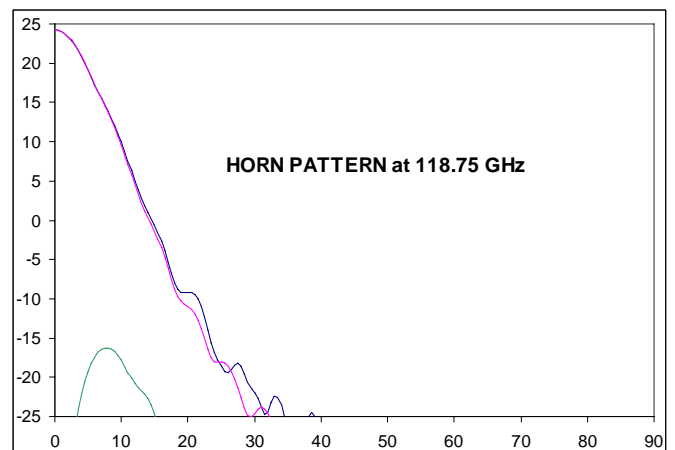
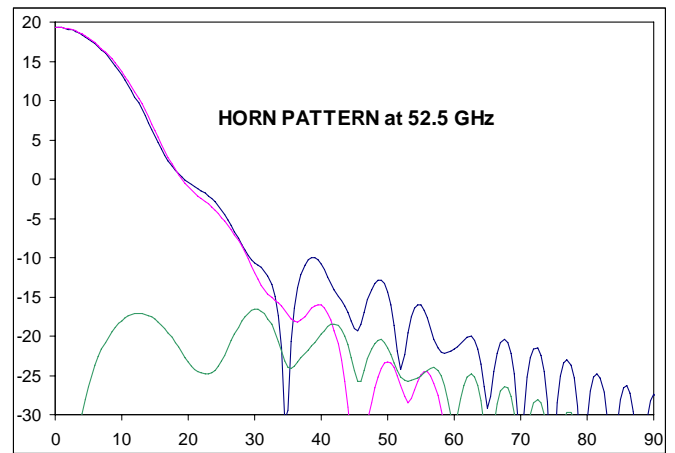


Figure 9: Radiation patterns of the single-depth corrugated horn with a hyperbolic profile optimized for footprint overlap

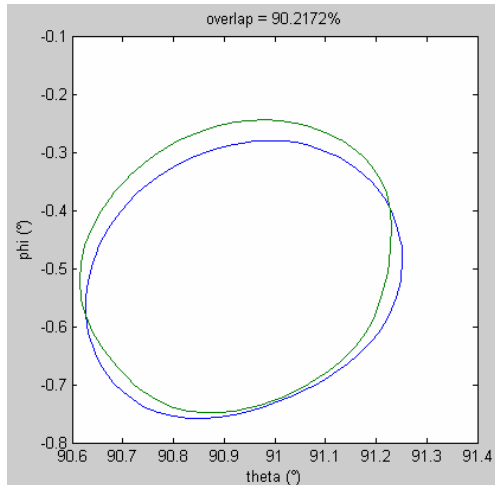


Figure 10: Both 52.5 & 118.75 GHz footprints of the antenna illuminated by the single-depth corrugated horn – 90 % of footprint overlap is achieved as required

#### 4 Antenna level performances

The antenna level performances have been computed for the preferred horn concept described here above and are presented in this section.

At the time this paper is being issued, the single-depth corrugated horn is not fully compliant at the edge of the 118 GHz band on the return loss (RL) and the cross polarization level. However this can be improved using a more appropriate mode converter. Further optimization of this part will have no consequence on the other antenna characteristics and will improve the situation for this point.

Channel	52.5			118.75			Spec
Frequency GHz	50	52.5	55	110.25	118.75	127.5	
FHPBW deg	0.53	0.54	0.56	0.6	0.57	0.65	<0.58°
FHPBW circular shape %	16.8	17.9	18.5	17.6	9.3	10.3	<20%
Footprint overlap %	90						>90%
Beam efficiency %	94.9	96.4	97	98.2	98.7	98.5	>95%
Cross-polar dB	-27.2	-26.8	-26.4	-28.5	-30	-19.4	<-25dB
Horn RL dB	-22.4	-23.6	-26.6	-20.8	-29	-23.8	<-28dB

Figure 11: Antenna level performance – optimised single-depth corrugated horn as feeder

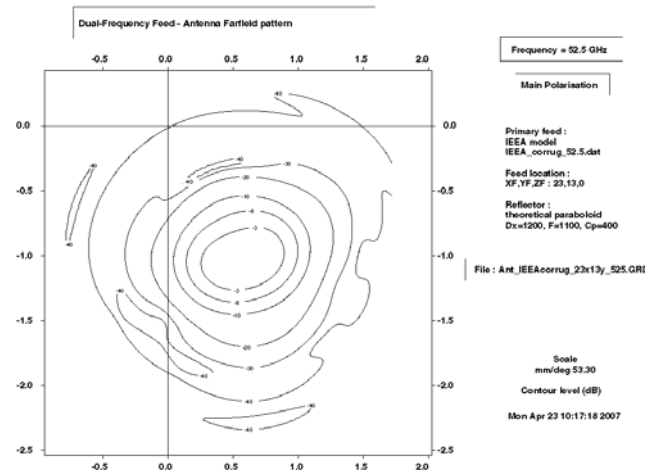


Figure 12: Antenna radiation pattern isolevel plot at 52.5 GHz (-3, -6, -10, -20, -30 & -40 dB levels)

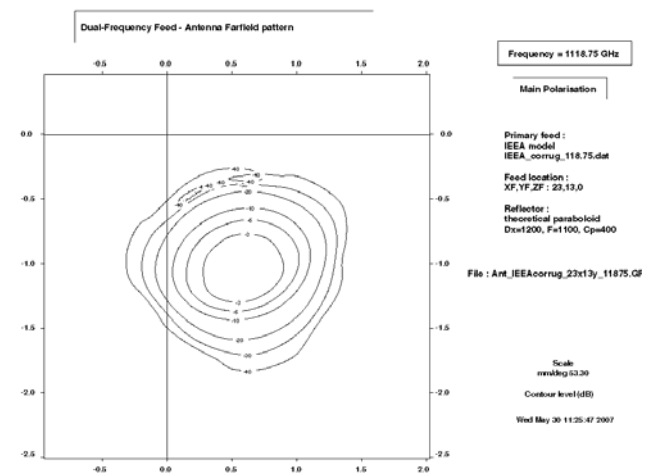


Figure 13: Antenna radiation pattern isolevel plot at 118.75 GHz (-3, -6, -10, -20, -30 & -40 dB levels)

The antenna radiation patterns are shown in Figure 12 & 13. The un-focused location of the DFF generates some distortion on the pattern but keep the antenna performance (footprint shape & overlap, beam efficiency, cross-polarisation) within acceptable limits as shown in Figure 11.

#### 5 Diplexer design & performance

##### Requirement:

The diplexer required frequency bands are 52.5 GHz +/- 2.75 GHz and 118.75 GHz +/- 9.0 GHz. The insertion losses must be <0.1 dB @ 52.5 GHz and <0.15 dB @ 118.75 GHz. The return losses at WG access have to be <-25 dB and <-28 dB at horn interface. The isolation must be >40 dB.

##### Principle:

To minimize losses, the higher frequency port is longitudinal and the lower frequency port is orthogonal wrt the horn axis as shown/depicted in the following figure. The frequency

filtering is performed by FSS at lower band and by the waveguide natural filtering at higher band.

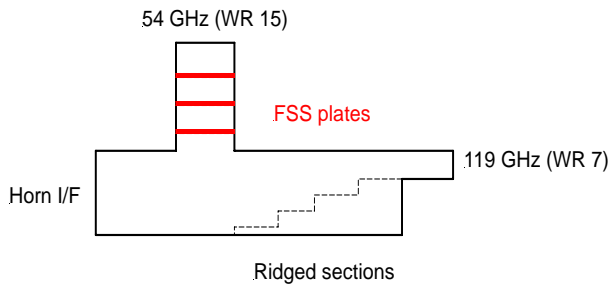


Figure 14: Diplexer principle

**Design:**

The FSS analysis and synthesis method are based on equivalent schematic extracted from full-wave EM simulation which fit well in case of constant incidence angle. In our case, the FSS being placed in a waveguide, the incidence angle is depending on frequency by the relation:  $\alpha = \arccos(\lambda_0 / \lambda_g)$ .

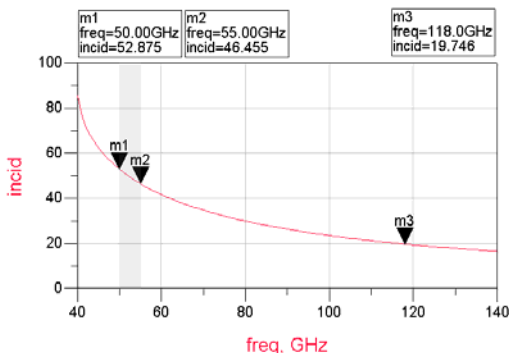
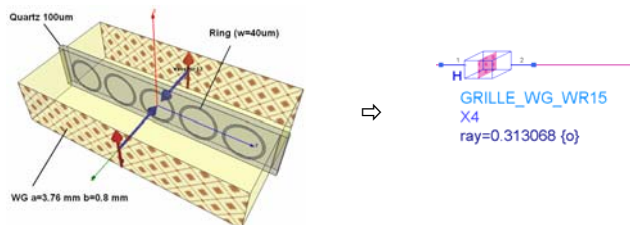


Figure 15: Incidence angle in a WR15 (3.76x1.88 mm) waveguide

LC model or stub model are not able to fit the frequency behaviour

To overcome this problem, we have used parametric EM simulations of FSS plate and then exported data to multidimensional S-parameter files. The method allows using S-matrix import from EM software with the possibility to optimize dimensions without the need of equivalent schematic.



HFSS parametric simulation export ADS circuit  
Figure 16: FSS model

Single ring and double rings FSS have been simulated for different ring radii and then exported to multidimensional S-

parameter files. A 3 plates filter has been optimized to reach the requirements.

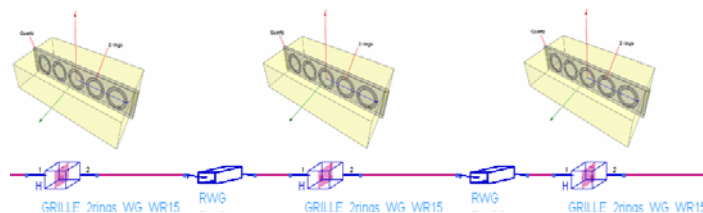


Figure 17: Three FSS plates necessary to reach the requirements

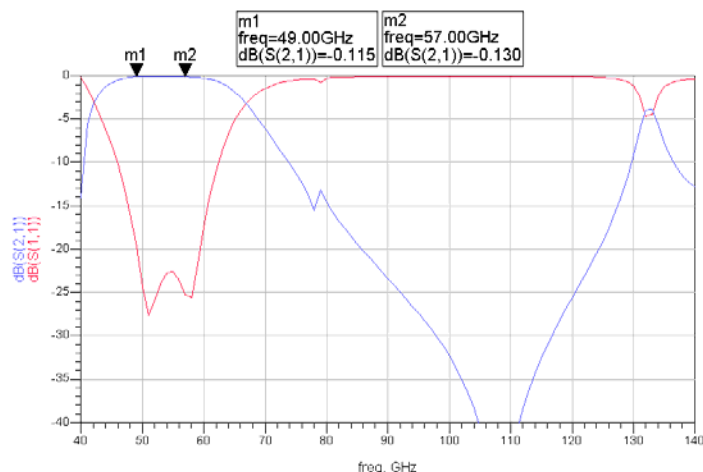


Figure 18: FFS band-pass filter in WG - ADS simulation from EM HFSS models

The last FSS plate has been incorporated in a Tee waveguide to be connected orthogonally. The higher frequency port has been reduced with ridged sections to fit the standard WG width.

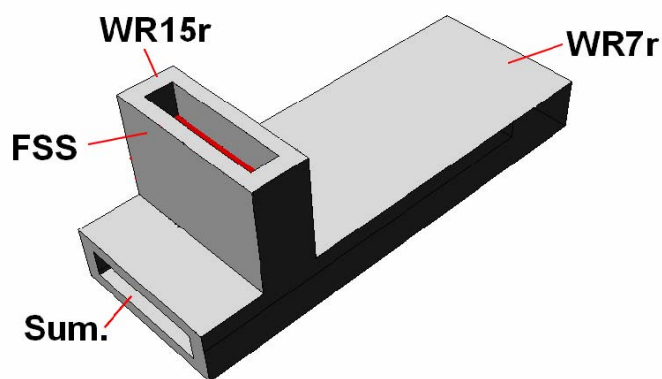


Figure 19: Final diplexer design (excluding rectangular to circular transition to horn)

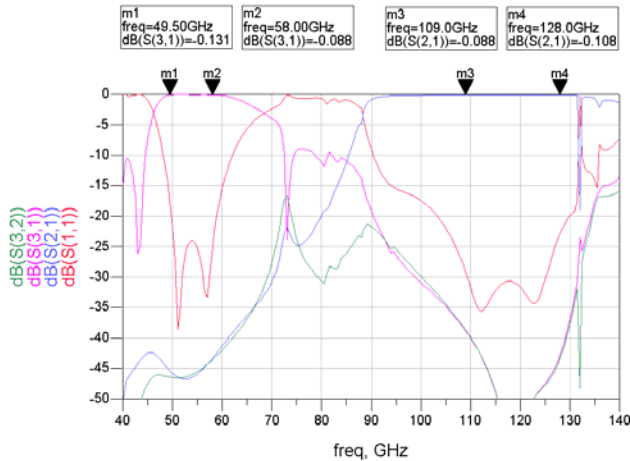


Figure 20: Final diplexer simulated results (excluding rectangular to circular transition to horn)

### Predicted performance:

52.5GHz insertion loss & RL	: 0.20 dB / -20 dB
118.75 GHz insertion loss & RL	: 0.15 dB / -20 dB
Isolation	: 38 dB
RL horn I/F	: -20 dB

## 6 Conclusion

A 54/119 GHz dual-frequency feed for illumination of an offset-fed parabolic reflector has been designed.

On horn side, the choice of the single-depth corrugated horn is obvious from the conclusions of the horn study summarised in section 3. The main performance at antenna level is achieved in both frequency bands, 50-55 & 110.25-127.5 GHz.

Further optimisation, including the reflector, are planned in the next detailed design & analysis phase in order to remove the slight remaining non-conformance.

On diplexer side, since the proposal phase and the beginning of the study, the concept including FSS within waveguide had very promising preliminary results compared to a classical filtering in waveguide. This is an innovative solution that has been pushed since the beginning for such an R&D activity. As for the horn, some RF characteristics will be improved (return loss, insertion loss) during the next phase in order to achieve the required performance level

## Acknowledgements

This R&D study is conducted by Astrium & IEEA under the ESA contract n° 20158/06/NL/JA.

## References

- [1] P.G Ingerson and W.V.T. Rusch, « Radiation from a paraboloid with an axially defocused feed », *IEEE Transactions on Antennas and Propagation*, vol. AP-21 no. 1, Jan.1973, pp.104-16
- [2] A.Berthon, R.Bills, "Integral Equations Analysis of Radiating Structures of Revolution", *IEEE Trans. Antennas and Propagation*, Vol. AP-37, no. 2, pp. 159-170, Feb. 1989
- [3] Sudhakar K. Rao and Minh Q. Tang, « Stepped-Reflector Antenna for Dual-Band Multiple Beam Satellite Communications Payloads », *IEEE Trans. Antennas and Propagation*, Vol. 54, no. 3, pp. 801-811, March 2006
- [4] Christophe Granet, « A Smooth-Walled Spline-Profile Horn as an Alternative to the Corrugated Horn for Wide Band Millimeter-Wave Applications », *IEEE AP*, vol. 52, no. 3, March 2004
- [5] E. Amyotte, Y. Demers, L. Martins-Camelo, Y. Brand, A. Liang, J. Uher, G. Carrier, J-P. Langevin, « High Performance Communications And Tracking Multi-Beam Antennas », *EUCAP 2006 proceedings*, November 2006
- [6] Xing-Hui Yin and Sheng-Cai Shi, « A Simple Design Method of Multimode Horns », *IEEE Trans. Antennas and Propagation*, Vol. 53, no. 1, pp. 455-459, Jan. 2005
- [7] Omid Sotoudeh, Per-Simon Kildal, Per Ingvarson, and Sergei P. Skobelev, « Single- and Dual-Band Multimode Hard Horn Antennas With Partly Corrugated Walls », *IEEE Trans. Antennas and Propagation*, Vol. 54, no. 2, pp. 330-339, Feb. 2006
- [8] Olver, *Microwave horns and feeds*, IEE electromagnetic waves series, Vol. 39
- [9] Noelia Ortiz Pérez de Eulate, Jorge Teniente Vallinas, Ramón Gonzalo García, Carlos del-Río Bocio, « Diseño de una Antena dual gaussiana de doble profundidad de corrugación »

(\*) Frequency Selective Surface